Reconnaissance on Liquefaction-induced Flow Failure Caused by the 2018 Mw 7.5 Sulawesi Earthquake, Palu, Indonesia

Risqi Faris Hidayat[1, *], Takashi Kiyota[1], Naoto Tada[2], Jun Hayakawa[3] & Hasbullah Nawir[4]

[1]Geo-disaster Mitigation Engineering Laboratory, Institute of Industrial Science, The University of Tokyo, 4-6-1 Komaba, Meguro-ku, Tokyo 113-8656, Japan
[2]Disaster Risk Reduction Expert, Japan International Cooperation Agency Indonesia Office, Sentral Senayan II, 14th Floor, Jalan Asia Afrika No. 8, Jakarta 10270, Indonesia
[3]Ministry of Land, Infrastructure, Transport, and Tourism, 2-3-1 Kasumigaseki, Chiyoda-ku, Tokyo, Japan
[4]Department of Civil Engineering, Faculty of Civil and Environmental Engineering, Bandung Institute of Technology, Jalan Ganesha 10, Bandung 40132, Indonesia
*E-mail: risqi-fh@iis.u-tokyo.ac.jp

Highlights:

- Long-distance flow failure on gently sloping ground.
- Sand boiling and subsidence due to soil liquefaction around the flow failure areas.
- Inundated freshwater and springs found even two weeks after the earthquake inside the affected areas, showing the possibility of the existence of a confined aquifer.
- A proposed mechanism of long-distance flow failure due to the presence of a confined aquifer.

Abstract. The M_w 7.5 Sulawesi Earthquake 2018 was a catastrophic disaster that resulted in large numbers of casualties. This study aimed to investigate the damages of liquefaction-induced-flow failure in three areas in Palu city, i.e. Petobo, Balaroa, and Jono Oge. It was found that this flow failure occurred on a large scale at a very gentle ground inclination, ranging from 1 to 3%. In order to gain an understanding of the soil conditions in these specific locations, Portable Dynamic Cone Penetration Tests were conducted in Petobo. The results showed that the soil layers in the affected area were in a loose state compared to the non-affected areas. Furthermore, some spots of freshwater inundation were recognized in Petobo and Balaroa, even two weeks after the disaster. Based on this evidence, a mechanism of liquefaction-induced-flow failure caused by a confined aquifer is proposed.

Keywords: *confined aquifer; gently sloping ground; liquefaction damage; lateral spreading; landslide; site reconnaissance.*

Received May 11th, 2019, Revised November 15th, 2019, Accepted for publication January 27th, 2020.

DOI: 10.5614/j.eng.technol.sci.2020.52.1.4

1 Introduction

On Friday evening, September 28, 2018, at 18:02:45 local time, an intra-plate earthquake (M_w = 7.5) was recorded around Donggala district, Palu, the central part of Sulawesi island, Indonesia. The United States Geological Survey in [1] informed that the epicenter (0.256 S and 119.846 E) was located 70 km from the northern part of Palu city at a shallow depth of around 20 km. The National Agency of Disaster Management in [2] reported that the earthquake triggered a tsunami in the coastal areas of Palu, Donggala, and Mamuju and liquefaction-induced-flow failure in some areas, such as Petobo, Balaroa, and Jono Oge. As a result, 2,101 people died, 4,438 people were injured, 1,309 people were missing.

The Palu-Koro fault is suspected to be the source of this earthquake. Bao, *et al*. [3] and Socquet, *et al*. [4] state that this earthquake was driven by the mechanism of super-shear rupture of the Palu-Koro fault. The strike-slip movement created the mainshock, as observed from its epicenter location, hypocentre depth, and the aftershock distribution (Figure 1).

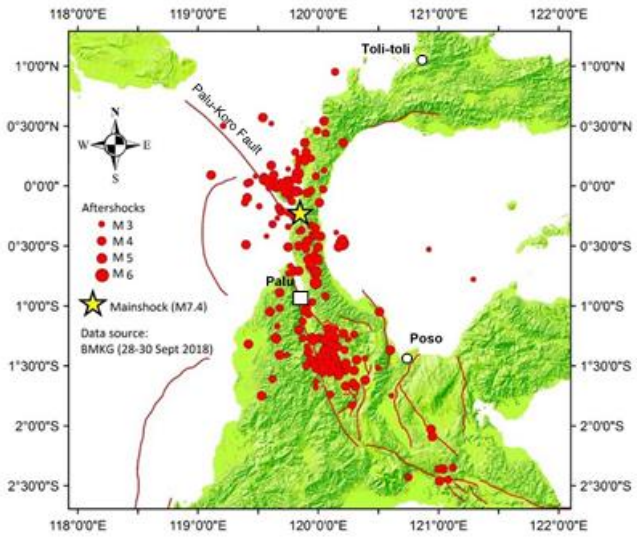

Figure 1 Epicenters of the Palu earthquake 2018 and the aftershock distributions (red dots) along the Palu-Koro fault in Central Sulawesi. (Edited from the Indonesian Agency for Meteorology, Climatology, and Geophysics in [5]).

This paper briefly discusses the local soil conditions to understand the mechanism and the extent of geotechnical damage due to this seismic event. The results of Portable Dynamic Cone Penetration Tests in Petobo are presented to illustrate the

soil layer characteristics. Relevant pictures display the aftermath conditions to show the damage encountered.

2 Geological Features of Palu City

Kadarusman, *et al*. [6], Bellier, *et al*. [7], and Watkinson, *et al*. [8] mention that Sulawesi Island is a complex tectonic collage that separates the converging Eurasian, Indo-Australian, and Philippines Sea Plates. This condition creates various geological conditions in each area, including in Palu city. As a result of the collision and interaction of these three plates, Sulawesi Island has several active faults, one of which is the Palu-Koro fault, which crosses Palu city and is assumed to have triggered the major earthquake in 2018. In addition to the uniqueness of its geological structure, Thein, *et al*. [9] notes that Palu city is composed of alluvial deposits in the valley, granite fragments in the northwest, granite and granodiorite rocks in the western to northern part, schistphyllitic rocks in the southern part, and molasses in the eastern part. Zeffitni [10] claims that the uniqueness of the geological structure (graben structure) in the Palu area defines its hydro-morphological condition, including the groundwater basin in this area. Petobo, Balaroa, and Jono Oge, which experienced a great extent of liquefaction-induced-flow failure, lie on these sediment layers.

3 Materials and Reconnaissance Method

Site reconnaissance was done from October 17th to 19th, 2018 with the main focus on investigating the geotechnical damage, particularly in three affected areas, as shown in Figure 2.

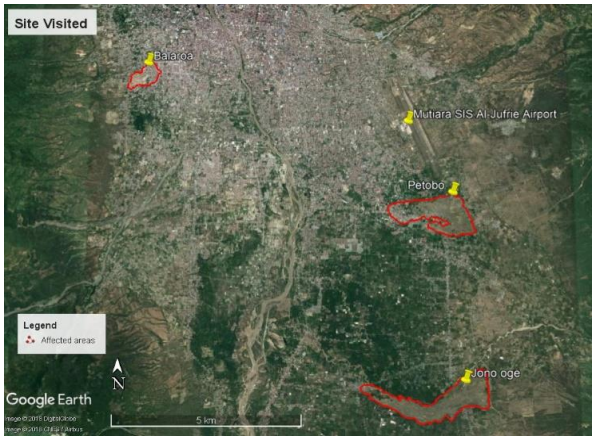

Figure 2 Sites visited during the investigation. The red border represents the affected zone of flow failure.

All the visited locations were accurately measured by GPS (Global Positioning System). A camera was also employed to capture real images of the conditions after the disaster. Satellite images from Google Earth, captured before and after the disaster, are shown to understand the extent of the disaster that occurred in the investigated places. Portable dynamic cone penetration tests (DCPT) were conducted in 4 spots at Petobo to obtain the in-situ ground penetration resistance inside and outside of the affected areas. The procedure for conducting this test followed the standard of the Japanese Geotechnical Society (JGS 1433-2012) in [8]. The equipment used is illustrated in Figure 3.

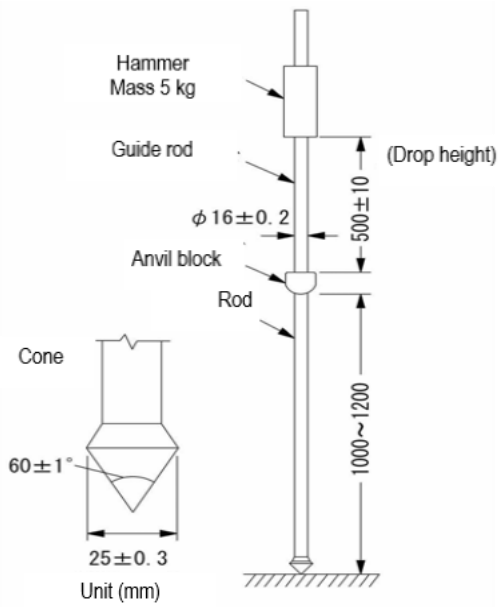

Figure 3 Portable dynamic cone penetration equipment.

4 Site Investigation Results and Discussion

By considering the scale of the affected area, this phenomenon was classified as liquefaction-induced-unlimited flow. Youd [9] remarked that liquefaction-induced-unlimited flow is a condition where the deformation in the liquefied state, the so-called flow deformation, is unstoppable.

At this state of liquefaction, the dilatancy-caused reduction of pore water pressure is insufficient to arrest the flow. Thus, the flow deformation will continue until the shear forces are reduced by several factors such as slope reduction to a state below the viscous shear resistance of the flowing material. The results of the investigation are summarized in Section 4.

4.1 Damages in Petobo

In Petobo, approximately 1920 buildings were reported collapsed and affected by the mass movement, with the majority being residential houses. The scope of the affected area was reported around 180 hectares, with a ground surface gradient of 3%. Figure 4 provides images of before and after the mainshock at Petobo, as captured by Google Earth. Points A, B, and C in Figure 4(b) show the location where Figure 5 was captured.

(a) Condition before the earthquake.

(b) Condition after the earthquake. Arrows show the direction of flow failure from the top to the bottom part.

Figure 4 Conditions at Petobo before and after the earthquake.

(a) Sand ejecta found in the non-affected area showing that liquefaction occurred due to the earthquake.

(b) Inundation at the bottom part of the debris zone found in Petobo, indicating that the groundwater table is high (Petobo).

Figure 5 Disaster evidence found at Petobo two weeks after the earthquake.

A witness living around the affected area informed that sand ejecta was produced after the shaking of the earthquake. It was also found that 30 meters from the crown, an irrigation channel lay parallel to the crown before the earthquake; after

the main shock, the water flow was reported to have vanished. Figure 5(a), taken at points A and C in Figure 4, displays the evidence of soil liquefaction; sand ejecta was found in several places in non-affected areas.

Even though little rainfall was recorded after the earthquake event, significant water inundation could still be observed in many parts, as shown in Figure 5(b), taken from the B point in Figure 4. In this area, the groundwater level was identified as shallow.

4.2 Damages in Balaroa

Compared to Petobo, the affected area in Balaroa was smaller (about 40 hectares). The number of buildings collapsed was over 1300 units. The topography was identified as gentle, with a gradient of 3-4%. The conditions before and after the main shock are illustrated in Figure 6. Points D and E indicate the location where Figure 7 was captured. A witness shared that the ground surface was undulating during the earthquake. After the shock, a mudflow started to appear and pushed houses to a lower elevation.

At the top, massive subsidence and tensile cracks were identified. Residential houses located 700-800 meters downstream were brushed up by the mudflow. From the center to the bottom part the houses were safe, yet inundated by the thick mudflow.

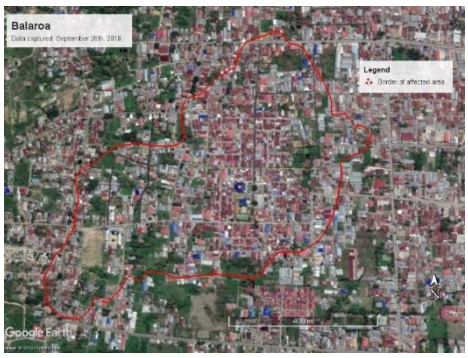

(a) Conditions before the earthquake.

(b) Conditions after the earthquake. The arrow shows the direction of mass movement from the top to the bottom part.

Figure 6 Conditions in the Balaroa area before and after the earthquake, captured by Google Earth.

Figure 7(a), taken at point E in Figure 6, shows sand ejecta on a house near the crown zone. Residents who have been living in the surrounding area for decades claimed that Balaroa has a shallow groundwater table. Like the condition at

Petobo, after the earthquake, some water inundation spots could also be observed in the middle part, around point D Figure 7(b).

(a) Sand ejecta found in the upper part, several meters from the crown (Balaroa).

(b) Some water inundation appeared after the event, showing that the groundwater level in this area is high (Balaroa).

Figure 7 Disaster evidence found at Balaroa during field reconnaissance.

4.3 Damages in Jono Oge

In Jono Oge, the affected area was around 210 hectares and the total number of damaged houses was about 500 units. The width of the affected zone was about 1 km, and the length around 3 km with an average ground gradient of 1%, the most gentle slope compared to the other two sites. Figure 8 provides an image of the conditions at Jono Oge before and after the earthquake. Points F and G indicate the location where Figure 9 was captured.

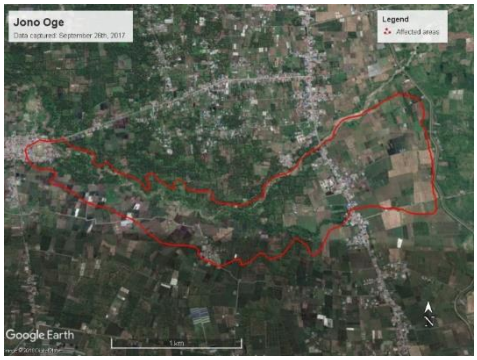

(a) Conditions before the earthquake.

(b) Conditions after the earthquake; the arrow shows the direction of mass movement from the top to the bottom part.

Figure 8 Conditions at Jono Oge area before and after the earthquake, captured by Google Earth.

According to witnesses living in the downstream area, the earthquake triggered a thick mudflow, which flowed for about an hour after the shock, immersing the houses on the leverage of the stream. From Figure 9(a), which was taken at point G in Figure 8, it can be inferred that the mudflow hitting the downstream area reached the structure of the temporary steel bridge. This led to the hypothesis that the thickness of the mudflow in this zone reached 1 to 3 meters.

It was also found that at point F, there was a house that still stood in the same position (Figure 9(b)) after the flow failure occurred, indicating that its foundation could resist the mudflow. Unfortunately, the mat foundation was not fully visible, but the part that was visible from the ground surface was around 70 cm.

(a) Dry mud on the bridge confirms that the thick mudflow passed by the bridge, immersing the houses in the downstream area (Jono Oge).

(b) Evidence of unmoved house to estimate the depth of the mudflow. Clay and silty deposits were found around this house. (Picture taken by T. Kiyota)

Figure 9 Disaster evidence found at Jono Oge during field reconnaissance.

4.4 Cracks in the Irrigation Channels

The irrigation channel 'Gumbasa' was located parallel to two of the affected areas, Petobo, and Jono Oge (Figure 10). Points H and I represent the location where Figure 11 was captured. Due to the earthquake, the channel was severely damaged.

During the earthquake, the channel was operated with a certain level of water, which had disappeard after the earthquake through large cracks in the channel body. A witness living close to the crown area in Jogo One stated that the irrigation channel was constructed in the 1980s to supply water to paddy and crop fields in the surrounding area. Before its construction, it was hard for people living in the downstream area to find groundwater, but one to two years after the construction people could quickly collect groundwater. It can be inferred that the presence of this channel affected the groundwater profile in the surrounding area.

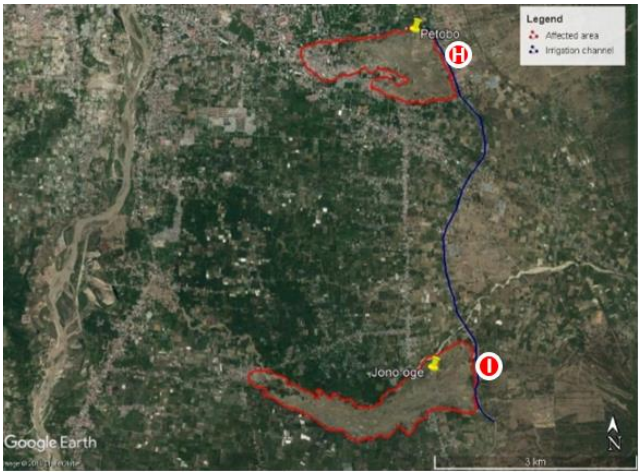

Figure 10 The irrigation section between Jono Oge and Petobo area (blue line).

(a) A big crack in the irrigation channel after the earthquake (Petobo).

(b) A big crack in the irrigation channel after the earthquake (Jono Oge).

Figure 11 Cracks were found along the irrigation channel. The water was dispersed after the earthquake event.

4.5 Dynamic Cone Penetration Test Results and Soil Classification

During the survey, portable dynamic cone penetration tests (DCPT) were conducted at four locations around Petobo, covering two points in the affected zone and the others in the non-affected zone. Figure 12 shows the locations of the test sites. By using the DCPT, the number of impacts necessary for the cone to penetrate 100 mm ground-depth are notated as Nd. This Nd value was then converted to an N-SPT value to represent the soil resistance as a more common variable. Takase and Sasada [11] summarized the empirical equations to convert Nd values to NSPT values for sandy (non-plastic) soil.

If $N_d < 4$, $N = 1.1+0.3N_d$ (1)

If $N_d > 4$, $N = 0.66N_d$ (2)

The DCPT conversion results are presented in Figure 3. From the test, the N-SPT value at point 1, which was several meters outside of the crown area, was relatively more dense than in the other spots. No evidence of liquefaction was observed around the spots. The groundwater level was identified at a shallow depth.

Figure 12 Locations of DCPT testing at Petobo, highlighted by red circles. Points 1 and 4 are outside the affected areas, while points 2 and 3 are near the crown area.

The soil condition in the crown area are represented by DCPT 2 and DCPT 3. In this location, up to a depth of 5-6 m, the N-SPT value was below 5, indicating that the soil was in a loose state. According to the Unified Soil Classification System, the sand ejecta samples taken at these points were classified as silt with low plasticity (ML), because the amount of fine content was more than 50% (Figure 14); the liquid limit (LL) was 28; and PI was 0 or non-plastic. The groundwater was found at a shallow depth. The combination of loose soil and shallow groundwater level possibly led to liquefaction due to earthquake shaking. DCPT 4 represents the soil condition at the bottom area. As this location is outside of the affected area, the N-SPT value was slightly higher than that of the affected locations. The groundwater level was identified at a shallow depth.

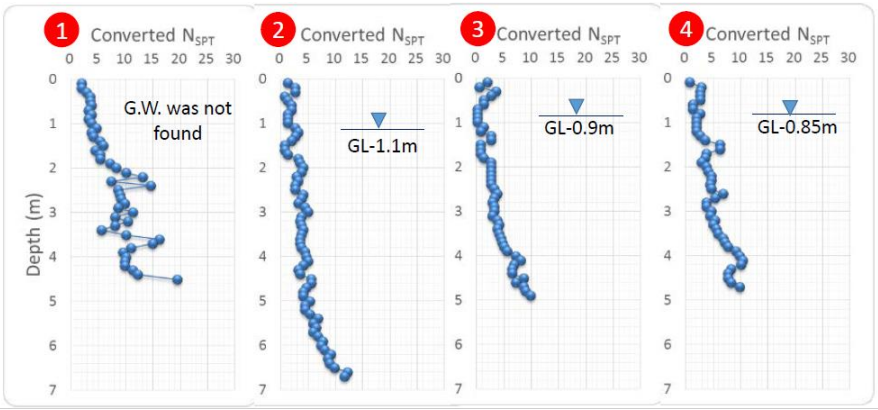

Figure 13 Converted N-SPT values from the DCPT tests. The groundwater level (GL) at points 2, 3, and 4 was low.

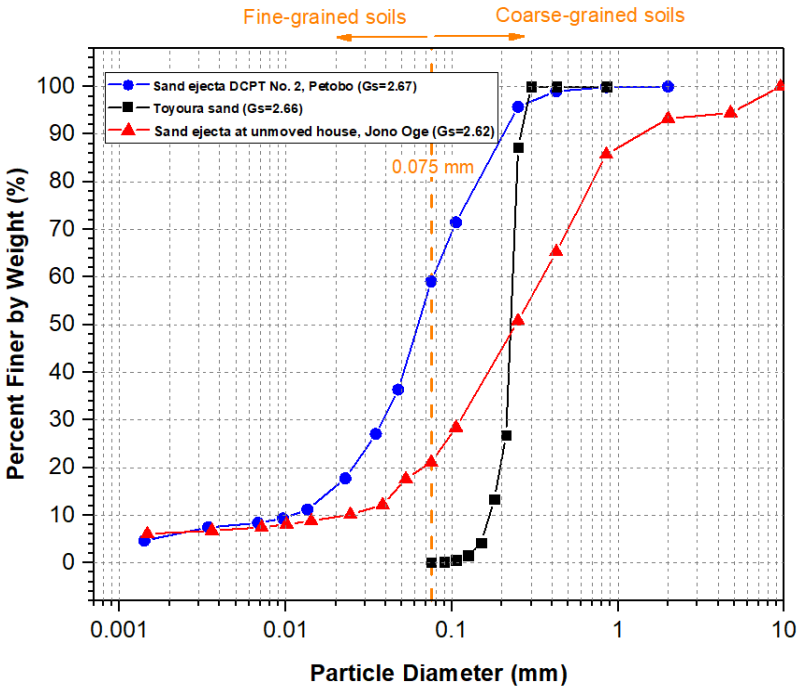

Figure 14 The grain size distribution of sand ejecta collected from Petobo and Jono Oge compared to Toyoura Sand. Both samples contained fine fractions.

After considering the extent of the damaged in the area, there is a strong hypothesis that there were external forces or pressures that caused the liquefaction-produced flow failure. Moreover, the topographic gradient of all the

affected areas can be categorized as a very gentle slope, ranging from 1 to 4%. In Balaroa, a local well-digger who had worked for decades in that place informed that before the earthquake happened, when a 6-meter-water pipe was inserted into the ground, the groundwater could eject at the surface to a height of about 0.5 to 1 meter. This information indicates that confined groundwater existed in Balaroa. It also supports the hypothesis that this type of liquefaction may be forced by pressure from confined groundwater.

5 Proposed Mechanism of Lateral Flow with Confined Aquifer

Bradley, *et al.* [12] analyzed the possibility that this lateral movement was promoted by the presence of the irrigation channel at Petobo and Jono Oge. However, this type of flow movement was also observed at Balaroa, where no irrigation channel existed and the ground inclination was also gentle. Considering this fact and information from the field reconnaissance, some hypotheses were formulated to understand the mechanism that caused this liquefaction-induced-flow failure, as illustrated in Figure 15.

It was estimated that in the three areas, unconfined as well as confined groundwater existed in the sandy soil layer. These layers were separated by a low-permeable soil layer, supported by the fact that a rice field existed in the three locations.

This condition is illustrated in Figure 15(a). When the earthquake occurred, the sandy soil layer was liquefied. This interpretation is in line with the results of the portable DCPT, which identified the loose sandy soil layer in this area. Simultaneously, the earthquake motion also disturbed the low-permeable-layer in the shallow layer (Figure 15(b)).

As a result, lateral flow and sand boiling occurred. After the earthquake shaking, the excess pore water pressure is usually dissipated and the soil layer becomes stiff again. However, in this condition the dissipation of excess pore water pressure may be restricted by the presence of a low-permeable surface layer (Figure 15(c)).

This restriction made the liquefaction state continue and the flow continued due to the upward osmotic pressure from the liquefied confined aquifer. This flow pushed the houses and all the infrastructure to a lower elevation and deposited them at the bottom of the slope. In the upper part, tensile cracks started to develop (Figure 15(d)). After reaching a large deformation, the liquefaction stopped and the induced-flow became stable. At some points, the seepage of groundwater from the confined aquifer can still be observed (Figure 15(e)).

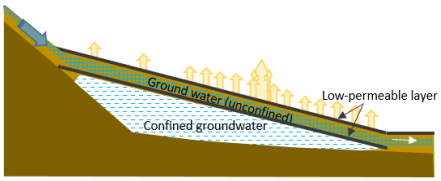

(a) Illustration of the initial conditions in the affected areas.

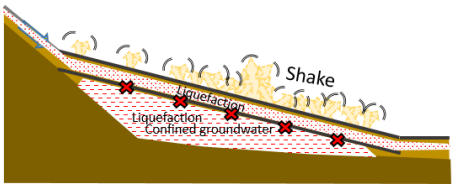

(b) The earthquake motion induced liquefaction in the sandy layer and disturbed the low permeable layer.

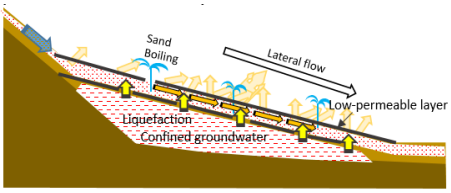

(c) Excess pore water pressure was unable to dissipate, so flow deformation continued to occur.

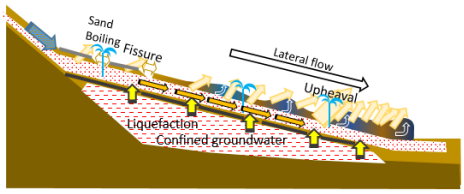

(d) The osmotic pressure from the confined aquifer made the flow continue and push all the buildings.

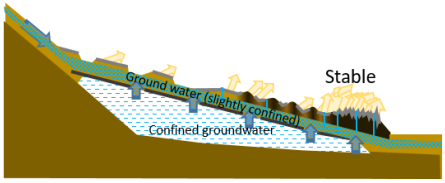

(e) The flow stopped and all the debris was deposited at the bottom part.

Figure 15 Proposed mechanism of the liquefaction-induced flow failure due to the earthquake.

6 Conclusion

The September 28, 2018 Sulawesi Earthquake affected several places in Sulawesi Island and brought a catastrophic disaster and great damage to Palu City. The Palu-Koro fault that crosses this city has been identified as the trigger of the earthquake.

Focusing on the damages due to liquefaction, three sites were visited, Petobo, Balaroa, and Jono Oge, where thousands of residential houses and casualties have been reported. The topography gradient of all affected areas was identified as gentle, with a gradient of 1 to 3%. Sand ejecta as evidence of liquefaction was

found in several places around the affected area. DCPT tests were conducted at four points in the Petobo area to identify the soil condition. In the affected area, the soil condition was identified as loose silt with a converted N-SPT value of less than 5 and the groundwater level was found at a shallow depth. Both factors imply that the liquefaction risk in this area is high.

The recovery of these three areas may be complicated. Relocation could be an option. Nevertheless, due to the unique topography and geological conditions in Palu city it is necessary to conduct a detailed geotechnical investigation and in-depth analysis relating to the liquefaction hazard to understand the possibility and to reduce the risk of future events.

Acknowledgment

The authors would like to thank Mr. Muhammad Rusli and the students from Tadulako University who have helped the authors in conducting the Portable DCPT Tests and Mr. Takanobu Kumagai from the Institute of Industrial Science, The University of Tokyo, for helping us to conduct the sieving test. Lastly, the first author expresses his gratitude to the Indonesian Endowment Fund for Education Agency for financially supporting his Ph.D study at The University of Tokyo.

References

[1] The United States Geological Survey, *Earthquake Hazards Program, The United States Geological Survey*, https://earthquake.usgs.gov/earthquakes/eventpage/us1000h3p4/executive, (October 28th, 2018).

[2] The National Agency of Disaster Management, *2018 Sulawesi Earthquake in Central Sulawesi*, The National Agency of Disaster Management, https://bnpb.go.id/geoportal.html, (November 13th, 2018).

[3] Bao, H., Ampuero, J. & Meng, L., *Early and Persistent Supershear Rupture of the 2018 Magnitude 7.5 Palu Earthquake*, Nat. Geosci., **12**, pp. 200-205, 2019.

[4] Socquet, A., Hollingsworth, J., Pathier, E., *Evidence of Supershear during the 2018 Magnitude 7.5 Palu Earthquake from Space Geodesy*, Nat. Geosci., **12**, pp. 192-199, 2019.

[5] Indonesian Society for Geotechnical Engineering, The National Research for Earthquake, & Ministry of Public Works, *Damages Associated with Geotechnical Problems in 2018 Palu Earthquake Indonesia*, The National Research Centre for Earthquake, Jakarta, 2018.

[6] Kadarusman, A., Leeuwen, T. van, & Sopaheluwakan, J., *Eclogite, Peridotite, Granulite, and Associated High-Grade Rocks from The Palu Region, Central Sulawesi, Indonesia: An Example of Mantle and Crust*

Interaction in A Young Orogenic Belt, in Proceedings JCM Makassar, 2011.

[7] Bellier, O., Sebrier, M., Beaudouin, T., Villeneuve, M., Braucher, R., Bourles, D., Siame, L., Putranto, E. & Pratomo, I., *High Slip Rate for a Low Seismicity along the Palu-Koro Active Fault in Central Sulawesi (Indonesia)*, Terra Nova, **13**(6), pp. 463-470, 2001.

[8] Watkinson, M.I., *Ductile Flow in the Metamorphic Rocks of Central Sulawesi*, The SE Asian Gateway: History and Tectonics of the Australia-Asia Collision, **355**, pp. 157-176, 2011.

[9] Thein, P.S., Pramumijoyo, S., Brotopuspito, K.S., Kiyono, J., Wilopo, W., Furukawa, A. & Setianto, A., *Estimation of Seismic Ground Motion and Shaking Parameters Based on Microtremor Measurements at Palu City, Central Sulawesi Province, Indonesia*, World Academy of Science, Engineering and Technology, International Journal of Geological and Environmental Engineering, **8**(5), pp. 308-319, 2014.

[10] Zeffitni, *Groundwater Potency in Palu Groundwater Basin Based on Hidromorfology and Hydrogeology Approachment* (in Bahasa Indonesia), Jurnal Geografi, **11**(22), pp. 97-106, 2013.

[11] Youd, T.L., *Liquefaction, Flow, and Associated Ground Failure*, U.S. Geological Survey, Virginia, 1973.

[12] Takase, M. & Sasada, M., *The Application of Portable Dynamic Cone Penetration Test to the Geo-Disaster Reconnaissance* (in Japanese), Japan Geotechnical Consultants Association Technical Forum 2013 in Nagano, pp. 64-65, 2013.

[13] Bradley, K., Mallick, R. & Andikagumi, H., *Earthquake-triggered 2018 Palu Valley Landslides Enabled by Wet Rice Cultivation*, Nat. Geosci., **12**, pp. 932-939, 2019.